JSEE Vol. 22, No. 3, 2020 DOI:10.48303/jsee.2020.249656

Research Paper

A New Configuration of Bearings by Optimum Design of Isolated Highway Bridges

Hamid Ganjehei[1], Panam Zarfam[2*], and Mohsen Ghafory-Ashtiany[3]

1. Ph.D. Candidate, Department of Civil Engineering, Science and Research Branch, Islamic Azad University, Tehran, Iran
2. Assistant Professor, Department of Civil Engineering, Science and Research Branch, Islamic Azad University, Tehran, Iran, *Corresponding Author; email: zarfam@srbiau.ac.ir
3. Professor, Structural Engineering Research Center, International Institute of Earthquake Engineering and Seismology (IIEES), Tehran, Iran

Received: 04/06/2021
Revised: 15/09/2021
Accepted: 23/02/2022

ABSTRACT

Highway bridges are amongst the most expensive, most widely used, and most vital infrastructures subject to the earthquake hazard. Seismic demand for bridges can be reduced by adding isolation systems. Lead-Rubber Bearing (LRB) isolators are widely used isolating devices whose optimal utilization studied in this article by using the Genetic Algorithm (GA). In this research, the analysis and design of deck-isolated bridges using Lead Rubber Bearings (LRBs) is carried out in accordance with the construction site, AASHTO criteria, and procedural rules for seismic bridge design. The LRB properties, along with the piers dimension selected as optimization variables. These variables' values applied in objective function using AASHTO design equations as constraints. Various pier heights and LRB placement scenarios regarded for assessing the sensitivity of optimum results. According to the results of the investigation, the research subject was repeated for not using LRB isolators in the side spans. Finally, a comparison of all the results showed that the larger LRB demands increased the effectiveness of LRBs in absorbing input vibrations and mitigating the bridge's seismic demand by about 20 to 50 percent. Also, it showed that it is more economical to exclude LRBs from abutment supports and limit their usage to the inner supports of the deck.

Keywords:
Isolated bridge; Lead Rubber Bearing (LRB); Optimization; Genetic Algorithms (GA)

1. Introduction

Over the last decade, the concept of using seismic isolation at the base of buildings has been proposed as a way to improve the performance for high-rise buildings, especially in seismic zones. Bridges are also considered as one of the critical structures in terms of efficiency after earthquakes, having an essential role as lifelines. In the past two decades, a few bridges have performed improperly after strong ground motions and have been damaged, which reveals the importance of research on bridges safety.

The base isolation equipment can be used to retrofit the critical structures and civil infrastructures, including seismic resistant design of bridges. LRB is one of the most widely used devices on bridges.

Regarding the application of base isolation in buildings, the effects of isolator and structure uncertainties in isolated and non-isolated reinforced concrete buildings are examined in several researches. Moreover, as one of the methods, reducing structural vulnerability has been confirmed in isolated structures by determining fragility curves (FC) after a large number of Incremental Dynamic Analysis (IDA) [1-2]. The same study is carried out

on isolated bridges carrying a box girder by Ramanathan et al. [3].

In addition, Shahria Alam et al. [4] carried out the seismic fragility assessment of a continuous multi-span isolated bridge in a survey and proved the reduction in fragility of bridge components. Moreover, they emphasized the importance of the role of bridge piers as well as the strong effectiveness of the LRBs.

In recent years, statistical-based design for the structural design of buildings has been performed using the base isolation system under nonlinear constraints [5-7]. In this regard, Jensen et al. [8] examined the reliability of structural nonlinear systems using statistical approaches and have demonstrated the high reliability of these systems.

To apply Genetic Algorithms (GA), Pourzeynali and Zarif [9] performed multi-objective optimization for isolated high-rise buildings and determined mass, stiffness and equivalent viscous damping of the isolation system to reduce the displacement of the buildings. In a study, Chisari et al. [10] specified the static and dynamic properties of isolated bridges using these algorithms. Subsequently, they obtained the behavioural specifications of the isolated bridges [10].

Ozdemir et al. [11] reviewed the environmental effects such as the temperature on the behaviour of LRBs in a box girder isolated bridge, with respect to the isolator's dimensions and specifications, and concluded that the effect of temperature on the isolation system should be considered during the design and implementation of these isolators. Hedayati Dezfuli and Sahria Alam [12] reviewed the strong effect of FRP-based elastomeric isolators on a bridge and reported that the effective horizontal stiffness and equivalent viscous damping of isolators are highly dependent on the shear modulus of the elastomer. Moreover, the vertical stiffness of isolators depends on the number of rubber layers and FRP thickness [12]. Lute et al. [13] found the beneficial effect of using genetic algorithms on the parameters considered including: the optimum bridge with minimal cost, the main tower height to span ratio and the main span to the side ratio. They applied the function of materials cost under the design constraints in an optimized cable-stayed bridge [13]. In a research, Fallah and Zamiri [14] determined the friction coefficient, mass of the base and the damping ratio of the device, with the objective of minimizing displacement and acceleration of the top floor and base displacement by multi-objective optimization of the sliding base isolation system using genetic algorithms.

Hameed et al. [15] studied the performance of the two-span bridge under a time-history based dynamic analysis. By considering the research variable, the peak ground acceleration to the peak ground velocity, they concluded that by increasing the PGA / PGV ratio, the displacement value and the LRB isolator forces decrease. Also, with an increase of the next variable, Q_d / W, the LRB isolator force is increased and its displacement is decreased. Based on the above, it was concluded that for sites with strong ground motions, it is best to use an isolator with small Q_d / W ratio, which is the characteristic strength, Q_d of the LRB isolator, normalized by the weight acting on the isolator [15].

By presenting ground acceleration records with accelerometers placed on an isolated bridge, Bessason and Haflidason [16] concluded that the isolators were effective in the longitudinal direction of the bridge and dissipated the energy, but were ineffective in the transverse direction of the bridge due to the small displacement of the super-structure.

By comparing the dynamic response of the isolated and non-isolated bridges under the near-fault ground motion, Liao et al. [17] concluded that the isolated bridge is suitable for the far-field ground motion, and in the isolated bridge with short and intermediate period, the displacement and base shear force values are strongly correlated to the PGV / PGA ratio and the energy of the ground motion.

Regarding the importance of the optimal design of LRB-isolated bridges as well as piers of bridges and according to the above review presented on this topic, the following objectives pursued by this study:

1. A comprehensive assessment on how various configuration parameters affect the optimum design obtained for LRBs and piers,
2. Complete incorporation of LRB design considerations including its effects on the vibration period and damping of the bridge and the demands undergone by the supporting piers, and

3. A study on the impact of various scenarios adopted for placing LRBs within the bridge structure.

The above-mentioned topics followed in this article by employing GA for the optimal design of a benchmark highway bridge using LRBs. The optimization process aims to design LRBs and the bridge piers following the AASHTO (LRFD bridge design specifications 1998) criteria by minimizing the equipment and material costs. The effect of bridge height on the optimization findings and the optimal bridge configuration is also assessed. Furthermore, the problem is solved a couple of times to appraise various scenarios for placing the LRBs on middle and side supports of the bridge deck.

2. Bridge Specifications

The preliminary bridge (before optimization) investigated in this study, has the highest number of constructed throughout the United States, 30923 bridges which are 18.9% of the total, according to the National Bridge Inventory (NBI) [18]. General specifications of this bridge which are called Multi Span Simply Support in the majority of the literature, or concisely expressed as MSSS, are presented below in Table (1) and Figure (1).

The width of each span is 15.01 m and is built using eight pre-stressed AASHTO type girders. The end span beams are AASHTO beams type I, borne on the abutments having an end pile at one end and a multi-column bent on the other end. Middle span utilizes AASHTO beams type III that are supported entirely by two multi-column bents. The other detailed characteristics of this bridge are obtained from a study on the existing bridges by Nielson [18] and are omitted here for the sake of brevity.

Table 1. Bridge material properties.

Item	Notation	Value	Unit
Shear Modulus of Rubber	G	1	MPa
Yield Stress of Steel	F_{ys}	240	MPa
Yield Stress of Reinforcement	F_y	414	MPa
Steel Modulus of Elasticity	E_s	2×10^5	MPa
Characteristic Strength of Concrete	f_c	28	MPa
Concrete Modulus of Elasticity	E_c	25267	MPa

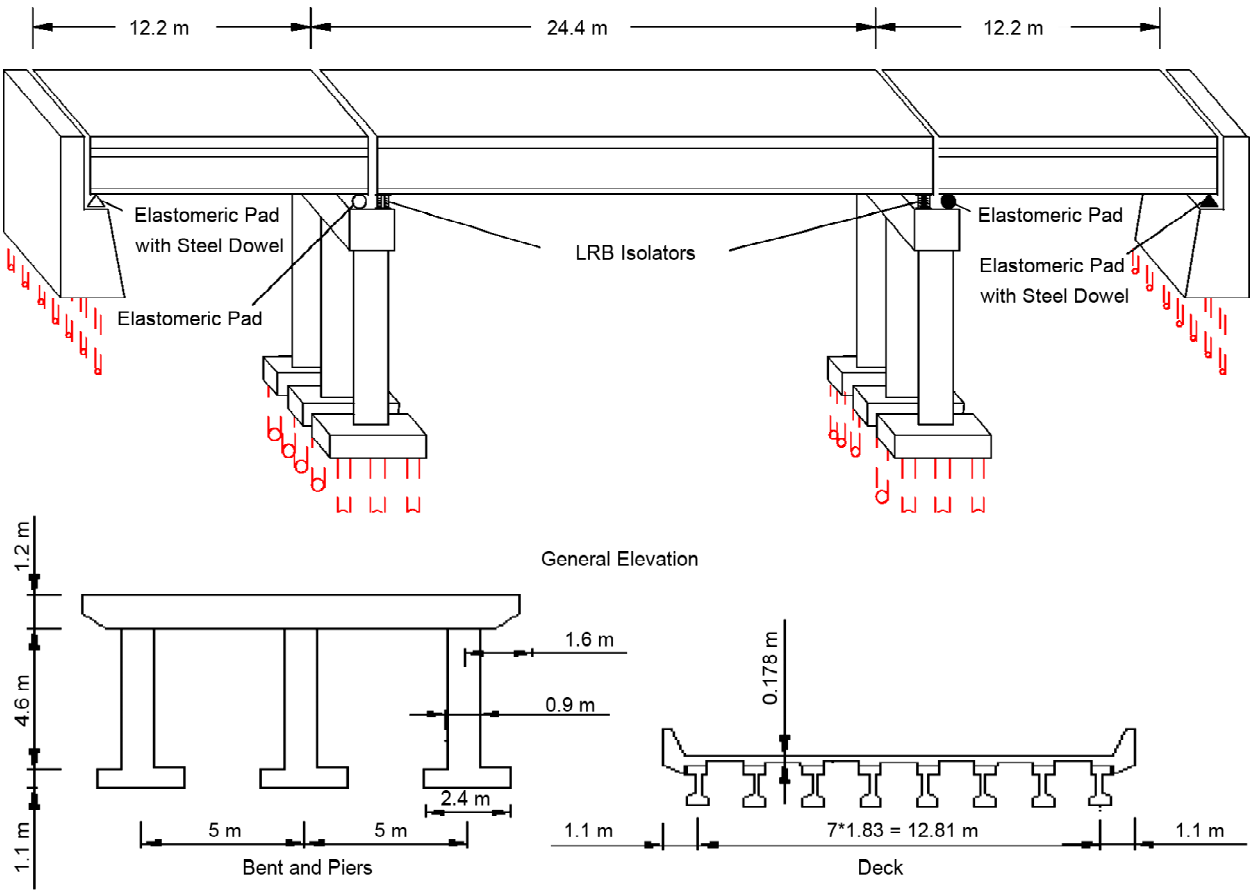

Figure 1. Layout of considered bridge [18].

3. Design and Modeling Method

The design of the bridge and the LRBs are performed following AASHTO LRFD (2014) as follows in the coming two sections.

3.1. General Bridge Design

For general design purposes, establishing a three-dimensional model of the bridge following the configuration is shown in Figure (1).

The earthquake loads are computed using the 5%-damped seismic design spectrum of AASHTO (1998). For adopting this spectrum, a soil type D assumed, and the values of PGA, S_S, and S_1 parameters are 0.35 g, 0.7899 and 0.2664 according to the bridge site location given in section 2. The resulting earthquake forces applied at two perpendicular directions. In addition to the earthquake, loads, dead, temperature, vehicle, shrinkage, and brake loads are also considered and combined following AASHTO specifications.

The initial modeling of the bridge employs the member dimensions and reinforcing details of bent and pier reported by Nielson [18]. Modal analysis of this model has led to the first and the second vibration periods of 0.62 and 0.42 seconds, respectively. These values are in agreement with the modal results obtained by previous research by Nielson [18] and can be regarded as a verification of the model established in this study.

The design of the piers follows ACI 318-14 (2014) specification for the design of reinforced concrete columns under compressive axial force and biaxial bending moments. The design of the bent girders, pre-stressed deck, and the abutments is only affected by the gravity forces and does not depend on the isolating system added to the bridge in this study. Thus, the related details are taken from the previous design by Nielson [18].

Additional AASHTO LRFD (2014) and FHWA-NHI 130093 (2014) [19] service limit state controls include average compressive stress of LRBs and their uplift under these stresses. LRBs' shear deformation, shear strain, and stability, as well as the minimum thickness of steel reinforcement are other parameters controlled under the same conditions.

The main effect of LRB isolators on the design of the bridge reflected in the model where the vibration periods of the bridge will increase and lead to a reduction of seismic force coefficients. Furthermore, the LRB damping will reduce seismic coefficient values by a reduction factor B_L, which applied to the design spectrum for modes with vibration period $T > 0.8T_{eff}$. The calculation of T_{eff} and B_L provided in the next section. In addition to the spectrum reduction, a lower level of inelasticity experienced by the isolated bridge than the non-isolated. According to AASHTO specifications, this effect reflected by halving the response modification factor, R, used for the design of the isolated bridge. Beside the impact of LRB isolators on the general design of the bridge, the design process will also engage in specifying the LRB characteristics. Details of this specification presented in the following section.

3.2. Design of the Isolating System

The LRB elements modeled on the piers and abutments supporting the deck for the seismic design of the deck-isolated bridge. An initial estimation is used for LRB stiffness so that the periods of the isolated system can be approximated to determine the spectral loading of the bridge. Spectral analysis is then performed to estimate the maximum displacement ($\Delta_{\max}$) and force ($F_{\max}$) demands of each LRB. The LRB strength, Q_d, is then estimated using Equation (1) and is used in conjunction with LRB demand values to approximate LRB damping, h. This is achieved using Equation (2) in which Δ_y and K_{eff} are the characteristic yield displacement and the assumed effective stiffness of the LRB. To account for LRB damping in the design of the bridge, the employed spectrum and the resulting bridge response (including $\Delta_{\max}$ and $F_{\max}$ of LRB) should be modified by the B factor computed using Equation (3). In this equation, S is spectral values. Upon this adjustment, the LRB's effective stiffness is updated through Equation (4), and the procedure repeated until converged pro-perties obtained for all LRBs.

$$Q_d = F_{\max} \tag{1}$$

$$h = \frac{2Q_d\left(\Delta_{\max} - \Delta_y\right)}{\pi K_{eff}\Delta_{\max}^{\ 2}} \tag{2}$$

$$B = \frac{S}{B_L} \quad where \quad B_L = \left(\frac{h}{0.05}\right)^{0.3} \tag{3}$$

$$K_{eff} = \frac{F_{\max}}{\Delta_{\max}} \tag{4}$$

In addition to the LRB mechanical properties obtained through the previous procedure, the physical properties of LRB should also be purchased for cost computing purposes. This starts by computing the lead core diameter, *dL*, using Equation (5) in which Q_d and *dL* are expressed in *N* and mm units, respectively.

$$dL = \sqrt{\frac{Q_d}{6.3585}} \tag{5}$$

By determining *dL*, the two other physical properties, the thickness of rubber layer (t_r) and the thickness of steel layer (t_s), can be best specified using Table (2) to reach the most economical LRB design.

Table 2. Recommended LRB thicknesses for steel and rubber layers.

d (mm)	t_r (mm)	t_s (mm)
d<=200	5	2
200 < d <=350	8	3
350<d<=650	12	4
650<d<=850	16	5
850<d<=1200	20	5

4. Genetic Algorithm-Based Optimization

For optimization of LRB design placed in bents and abutments, GA codes of MATLAB R2016a software are used [20]. The process of the minimization problem is expressed as follows:

- Assuming General Characteristics of LRB including lead shear yield stress, isolator shear modulus and steel yield strength.
- Calculation of the design spectrum related to the bridge construction location in the USA with PGA and S_s and S_1 coefficients, and soil type *D* based on AASHTO (limit states).
- Three-dimensional modeling of the bridge in CSi bridge software (Ver. 16) [21] assuming an initial lateral stiffness of LRB and conducting the gravity analysis. Subsequently, spectral analysis of the considered bridge is done to determine the displacement of the isolator, and then for each chromosome in the GA loop, this spectral analysis is corrected once based on the isolator damping (B_L coefficient and period of the isolated bridge $T > 0.8T_{eff}$). The final output of the isolators' displacement at bents and abutments is obtained with converged forces of isolators.
- Performing the optimization of LRB design by using GA in MATLAB software by taking into account seven variables, six of which: the number of rubber layers (n_r), the overall diameter of isolator (*d*), diameter of lead (*dL*) used for the middle isolator (bent) and side isolator (abutment) in the range of lower and upper bounds as follows: the number of rubber layers 2 and 10, the overall diameter of isolator 200 and 1000 mm, diameter of lead to diameter of isolator ratio 0.1 and 0.3 and the last variable is diameter of reinforced concrete pier (D_c) in the range of lower and upper bound of 900 and 1300 mm. Moreover, the LRB design constraints are assumed according to the AASHTO and also function of minimizing the cost of materials and construction prices of LRB and reinforced concrete piers.

  Reinforced concrete piers have been designed similar to the reinforced concrete columns under the compressive axial force and biaxial bending moment values due to the bridge deck loads. The spectral analysis is conducted in accordance with the site design spectrum.

  With respect to the defined problem, the objective function is the total cost of the isolator including the cost of materials and the cost of construction displayed as Equation (6).

$$f(x) = \left[(P_{LRB}.h_{LRB}.A_{LRB}) + (P_s.W_s) + P_c.D_c^2.\pi/4\right] \tag{6}$$

  where P_{LRB} is *LRB* isolator price (32 US$ per dm^2), P_s is reinforcement price (0.40 US$ per kg), P_c is concrete price (24 US$ per m^3), h_{LRB} is total height of LRB (mm), Ws is total weight of reinforcement (kg), A_{LRB} is total cross section of *LRB* (mm^2) and D_c is diameter of concrete pier (mm).

  With respect to the defined problem, the con straints functions are based on the design formulas of the AASHTO LRFD (2014) and FHWA-NHI 130093 including control of the

average compressive stress at the service limit state, uplift under average compressive stress at the service limit state, shear deformation under the average compressive stress at the service limit state, control of shear deformation, shear strain, the stability of elastomeric bearings, the minimum thickness of steel reinforcement and seismic controls of seismic LRB isolators.

- The objective function is calculated for each set of assumed variables on each chromosome, if convergence conditions and design constraints have been passed. Then, based on the assumptions of the genetic algorithm described in the following paragraph, it is repeated to obtain the optimal economical solution.

For the implementation of GA, the input data is used as follows: Constraint tolerance is equal to 1e-3 that is the software default and used to determine the feasibility with respect to nonlinear constraints. Uniform Creation Function selected as not to miss the initial range, scattered Crossover Function to create a random binary vector. Crossover Fraction is equal to 0.8, which is the software default and is the fraction of the population at the next generation, excluding elite children. Population Size is equal to 50 as the software default and according to the number of variables. Elite Count is equal to 0.05x Population Size as the software default to specify the number of individuals in the current generation are guaranteed to survive into the next generation. Number of variables is equal to 7 and Max Generations is equal to 21 according to the number of variables for reducing problem size. Function Tolerance is equal to 1e-6, which is the software default and is used for algorithm stops if the average relative change in the best fitness function value. The Initial Penalty is equal to 10 that is the software default. Augmented lagrangian as Nonlinear Constraint Algorithm, which is the software default to solve a nonlinear optimization problem with nonlinear constraints, and Penalty Factor equals to 100 as the software default, which is described in the following paragraph.

Using the high optimization parameters, the optimization solutions were strongly obtained.

The algorithm of research implementation is presented in Figure (2).

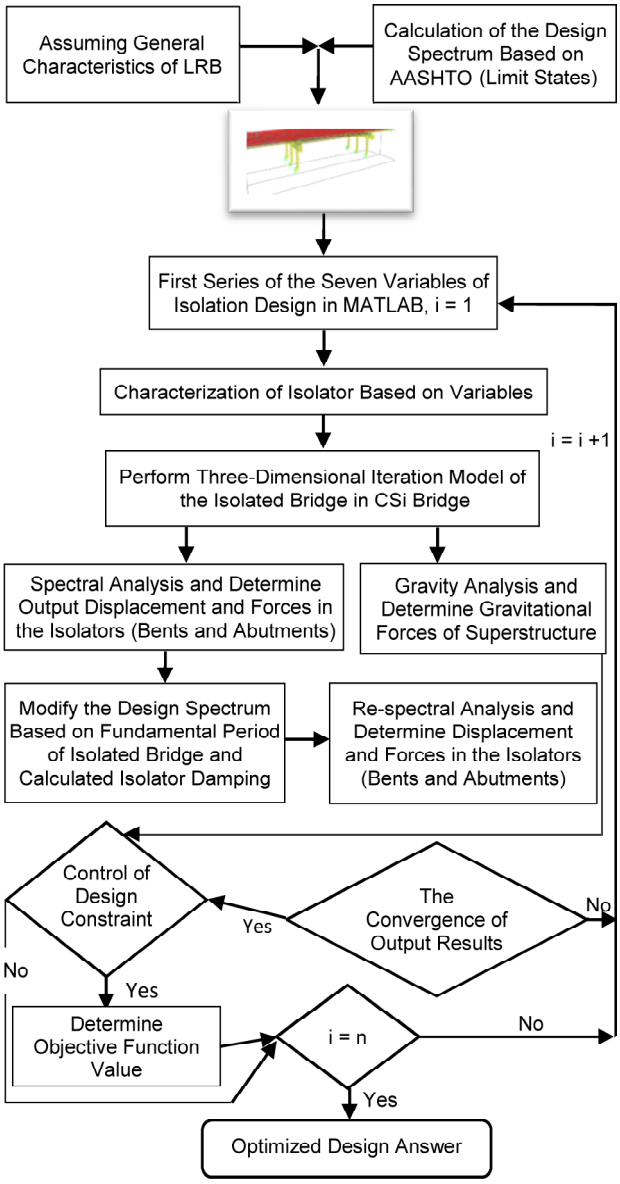

Figure 2. Algorithm of research implementation.

It should be said that, for cases in which a structure meets all design constraints, the cost value itself can be used for manipulating the x vector so that a more optimal solution achieved. By weakening the structures, on the other hand, some cases will provide unacceptably low costs by not fulfilling some of the constraints. To prevent the identification of these structures as the right solutions (due to their low costs), the real cost of these structures should be amplified by a penalty factor that is greater than unity. This factor should approach zero as the structures get closer to the constraint limits and have to grow by further weakening of the structure. A mathematical implementation of this concept for applying the design constraints on the optimization process is obtained by introducing an equivalent cost, costeq. This equivalent cost is

computed by multiplying the cost value consequent to an x vector by a penalty factor, following Equation (7).

$$cost_{eq}(x) = penalty \times cost(x) \quad (7)$$

$$penalty = 1 + 100 \times \sum_{all\ constraints} k_i \quad (8)$$

According to Equation (8), the penalty factor is 100 times the sum of partial penalty factors, denoted by k_i, computed for different constraint equations. Each k_i is zero when the related constraint is met and becomes unity on the constraint's boundary limit. Upon violating the constraint boundary, k_i proportionally increases from unity. The 100 factor emphasizes the satisfaction of constraints in obtaining the optimal solution. The suggested solutions approach rapidly toward the space in which design constraints are satisfied using this factor.

5. Numerical Results

5.1. Results for the Use of Side Spans and Middle Span LRBs

Three-dimensional finite element models of deck-isolated bridges using LRBs are provided by CSi Bridge 2014 (ver. 16) software [18]. Modal analysis of the entirely deck-isolated bridge having a net pier height of 4.60 m (short), using CSi Bridge software, shows that the period of the first mode is approximately 0.73 seconds in the first iteration with LRB specifications and dominant movement in the longitudinal direction. The second mode is a transverse mode having a period of 0.56 seconds.

Also, to investigate the effect of height on the optimal isolator, the net pier heights (h_c) were considered as 4.60, 7.10 and 9.60 m that have been named short, medium and long in this research. Based on the provisions of reference [18], the pier's height of 4.60 m was selected. In order to consider the effects of pier's slimming on the analysis results, as well as considering the implementation issues

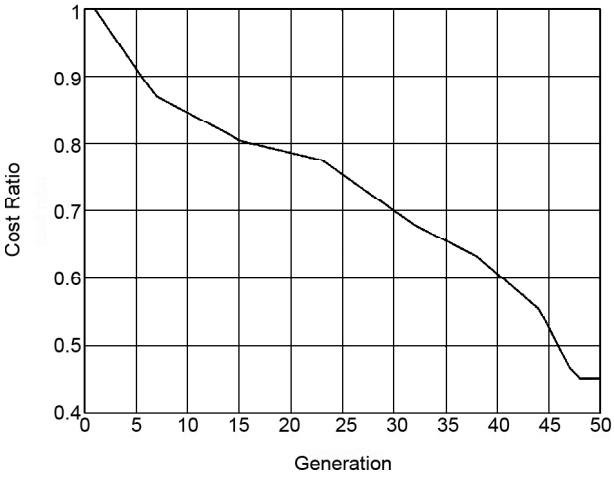

Figure 3. The changes in bridge equivalent cost throughout generations.

of formworks, incremental steps of 2.50 m were considered to increase the height of the piers.

The trend of changes in the equivalent cost values during the optimization procedure presented in Figure (3) for a typical bridge. For extracting these curves, in each generation of bridge produced by GA, the genome (bridge) with the lowest equivalent cost found. This cost is then depicted along the y-axis, while the x-axis shows the number of gener-ations to reveal the gradual approach of the expenses toward an optimal value. As the genomes become optimized, they move inside the allowable area imposed by design boundaries. Thus, the penalty factors related to violation of these criteria approach zero, and the initially high equivalent costs will contact the actual bridge cost.

The main output results, including the optimized dimensions of middle and side LRB isolators, along with the piers diameters are summarized in Table (3). The feature values of optimized LRB isolators and stiffness ratio of abutment to bent are summarized in Table (4).

As it is noticeable in Tables (3) and (4), for middle span optimum LRB isolators (bent), increasing the piers height resulted in the increase of the effective stiffness of optimum LRB isolators,

Table 3. Optimum dimensions of research variables.

h_c (m)	Middle Span (Bent) LRB			Side Span (Abut.) LRB			D_c (cm)
	d (mm)	n_r	dL (mm)	d (mm)	n_r	dL (mm)	
4.60	450	9	67.5	300	3	60	130
7.10	350	5	35	300	4	75	130
9.60	350	6	70	300	4	90	130

Table 4. The feature values of optimized LRB isolators and stiffness ratio of abutment to bent optimum LRB isolators.

h_c (m)	Middle Span (Bent) LRB			Side Span (Abut.) LRB			$\frac{K_{eff;Side}}{K_{eff;Mid}}$
	Q_d (kN)	K_u (kN/mm)	K_{eff} (kN/mm)	Q_d (kN)	K_u (kN/mm)	K_{eff} (kN/mm)	
4.60	28.97	15.83	1.82	22.89	31.1	3.56	1.95
7.10	7.79	26.19	2.7	35.77	22.78	2.93	1.09
9.60	31.16	21.17	2.45	51.5	22.11	3.29	1.34

LRBs diameter and height reduction and number of rubber layer reduction. Also it can be concluded from Table (3) that by increasing the piers height, the stiffness of the middle span optimum LRB isolators with medium height is maximum.

Regarding the optimum LRB isolators of the side spans (abutment), increasing the piers height resulted in the slightly reduction of effective stiffness of optimum LRB isolators, while it increased the diameter of the lead core, LRBs height and number of rubber layers.

In piers with the same height, the following results are observed:

- A significant reduction in the diameter of side spans optimum LRB isolators compared to the middle span.
- Increase in the diameter of lead core side spans optimum LRB isolators with the exception of short piers height.
- Numerous rubber layers of the middle span optimum LRB isolators compared to the side spans.
- Increase in the cross section of middle span optimum LRB isolators.
- Increase in the height of the middle span optimum LRB isolators
- The same values for piers diameter.

All the results listed above are verified in Table (4) by the stiffer side spans optimum LRB isolators compared to the middle span optimum LRB isolators.

Finally, the effective stiffness values of the side spans optimum LRBs to middle span ratio are provided in Table (4). The numbers shown in the table indicate a decrease in the stiffness ratio as pier height increased.

As it is evident from Table (4), at the middle span of bridge, effective stiffness, K_{eff}, of the optimum LRB is maximum for the moderate pier height of 7.1 m. According to the bridge geometry, the LRB and pier elements work in series with each other. This means that these members resist equal shear forces while attracting lateral deformations in the proportion of their flexibilities. Therefore, for a constant lateral force applied to a LRB-pier system, the value of the lateral deformation undergone by LRB depends on its lateral flexibility with respect to the underneath pier. This deformation, on the other hand, has a reverse correlation with the effective stiffness of LRB, according to Equation (4). Regarding these facts, an increase in lateral deformability of the pier will cause the maximum deformation of LRB to decrease and thereby its effective stiffness to increase. Because the maximum LRB stiffness has coincided with the moderate pier height, it can be said that both short and long piers have larger deformability than moderate-length ones. This is in agreement with known structural analysis facts. For long piers, the small flexural stiffness is responsible for the extra deformability of the pier. For short piers, however, it is the great overturning moment caused by the lateral force that leads to an enlarged lateral deformation of the pier. The piers with moderate lengths are thus expected to intervene in the two extreme cases and provide the lowest deformability. The mentioned increase of K_{eff} at middle spans is also responsible for the reduction in pier's diameter, LRBs' diameter and the number of rubber layers.

For the side LRBs, a reverse trend observed, and the effective stiffness of LRB minimized for the pier with moderate length. As stated above, the lateral stiffness of such piers is more substantial, and they absorb a higher proportion of lateral forces induced on the bridge. Therefore, the lateral reaction of abutment LRB decreases to account for the higher resistance in the middle parts. This reduced LRB force will, in turn, lead to a reduced effective stiffness according to Equation (4). This observation can also be made by considering the side-to-middle LRB stiffness ratios provided in the last column of Table (4).

According to these values, a more significant pro-

portion observed for short piers indicating that shortening the pier is more effective in reducing its lateral stiffness than enlarging it. Again, the changes in the physical properties of middle LRBs follow the stiffness trend and need not interpreted separately.

The same piers diameter values indicate the optimization performance with increasing stiffness of the side isolators compared to the middle and slight lateral displacement in the side span.

In Table (5), values of the reinforced concrete piers design forces are summarized in addition to the designed reinforcement percentages for each pier. As displayed in this table, by increasing the height of middle and side piers, the axial force and biaxial bending moment values are increased. Even the biaxial bending moment in the piers with medium height is greater than long. Similarly, the same results are observed for the percentage of designed reinforcement of piers. For piers with medium height, a greater percentage of cross-sectional reinforcement is calculated compared to the other two heights.

On the other hand, for all three heights studied in this research, the values of design forces are greater at the side piers compared to the middle piers.

The maximum displacement values of optimized LRB isolators and yield displacement values of optimized LRB isolators are summarized in Table (6). As shown in this table, by increasing the piers height, the maximum displacement of optimized isolators is reduced with the exception of medium side piers height. This is in contrast to the values of yield displacement of LRB isolators increased for side piers and almost reduced specially for medium middle piers, which is consistent with the characteristics of strength and isolator's optimum stiffness values.

5.2. Results for the Use of Middle Span LRBs

Comparing the optimal LRB properties obtained for the side and middle spans lead to the conclusion that lower LRB properties required at the side spans. It can identify that the lower bound values are selected for optimization variables by the algorithm considering the side LRB properties. This implies that excluding the LRBs from side spans (abutments) may lead to further reductions in the cost of the optimum solution. The optimization process was repeated another time to examine this, and the optimum values reported in Tables (7) and (8).

Table 5. The piers design forces and percentage of the piers designed reinforcement.

h_c (m)	Middle Pier			Side Pier		
	P_u (ton)	M_u (t.m)	Pier Rebar (%)	P_u (ton)	M_u (t.m)	Pier Rebar (%)
4.60	-177.23	407.2	0.0113	-187.68	417.77	0.0116
7.10	-206.95	563.79	0.0172	-288.71	607.05	0.0179
9.60	-218.19	533.41	0.0158	-306.61	583.85	0.0167

Table 6. The deck maximum displacement of optimum isolators and isolators yield displacement values.

h_c (m)	Middle Span (Bent) LRB		Side Span (Abutment) LRB	
	Maximum Horizontal Displacement (mm)	Isolator Yield Displacement (mm)	Maximum Horizontal Displacement (mm)	Isolator Yield Displacement (mm)
4.60	120.68	2.03	50.62	0.82
7.10	98.01	0.33	55.19	1.75
9.60	92.54	1.63	47.59	2.59

Table 7. Optimum dimensions of research variables.

h_c (m)	Middle Span (Bent) LRB			D_c (cm)
	d (mm)	n_r	dL (mm)	
4.60	350	6	105	90
7.10	400	8	100	110
9.60	350	7	87.5	100

Table 8. The feature values of optimized LRB isolators.

h_c (m)	Middle Span (Bent) LRB		
	Q_d (kN)	K_u (kN/mm)	K_{eff} (kN/mm)
4.60	70.1	20.06	2.94
7.10	63.59	13.5	2.09
9.60	48.68	17.72	2.3

As it is noticeable in Tables (7) and (8), for middle span optimum LRB isolators (bent), increasing the piers height resulted in reduction of the effective stiffness of the optimum LRB isolators, almost similar to the LRBs diameter and diameter of the lead core and number of rubber layers. Also, it can be concluded from Table (7) that by increasing the piers height, the stiffness of the middle span optimum LRB isolators with medium height is minimum.

Values of the system effective period are 0.84 sec for piers with 4.60 m height (short), 0.99 sec for 7.10 m height (medium) and 0.96 sec for 9.60 m height (long).

In Table (9), the values of the reinforced concrete piers design forces are summarized in addition to the designed reinforcement percentages for each pier. As displayed in this table, by increasing the pier height at middle piers, the axial force and biaxial bending moment values are increased and at side piers decreased. Even the biaxial bending moment in the piers with medium height is greater than long. Also, by increasing the height of middle and side piers, the piers optimum diameter is increased. However, the percentage of designed reinforcement of piers is reduced, especially for piers with medium height.

On the other hand, for long heights studied in this research, the values of design forces are less at the side piers compared to the middle piers.

The maximum displacement values of optimized LRB isolators and yield displacement values of optimized LRB isolators are summarized in Table (10). As shown in this table, by increasing the piers height, the maximum displacement of optimized isolators is increased. The values of yield displacement of LRB isolators are decreased with the exception of medium piers height.

According to above tables, similar observations can be made for the relationship between optimum effective stiffness of LRB and the pier height. The optimal costs obtained in this case are remarkably less than those obtained by the inclusion of side LRBs. The full costs obtained at the optimum state are shown in Table (11) to evaluate this issue further.

The effect of design assumption (inclusion or exclusion of side LRBs) and the bridge height on piers' force demands graphically evaluated in Figures (4) and (5). According to the figure, the exclusion of side LRBs has led the major design forces to transfer to the abutments.

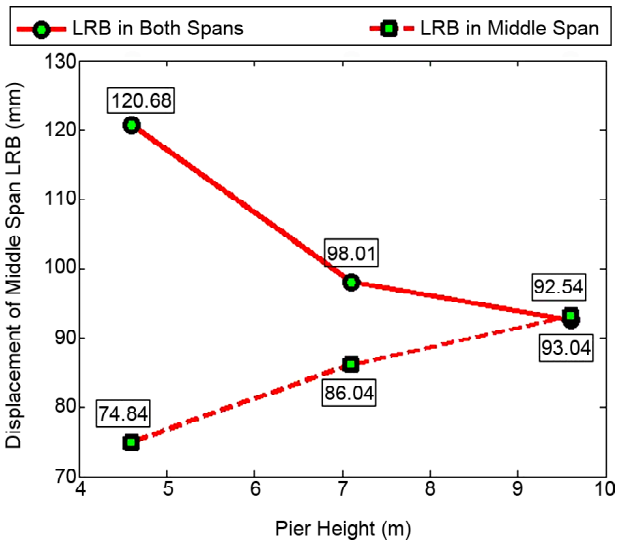

Figure 4. The displacement of middle span LRBs.

Table 9. The piers design forces and percentage of the piers designed reinforcement.

h_c (m)	Middle Pier			Side Pier		
	P_u (ton)	M_u (t.m)	Pier Rebar (%)	P_u (ton)	M_u (t.m)	Pier Rebar (%)
4.60	-220.88	99.53	0.0029	-221.83	118.14	0.0051
7.10	-221.69	110.03	0.001	-219.35	121.21	0.0014
9.60	-249.11	102.95	0.001	-90.22	70.55	0.0023

Table 10. The deck maximum displacement of optimum isolators and isolators yield displacement values.

h_c (m)	Middle Span (Bent) LRB	
	Maximum Horizontal Displacement (mm)	Isolator Yield Displacement (mm)
4.60	74.84	3.88
7.10	86.04	5.24
9.60	93.04	3.05

Table 11. The total cost of isolators, concrete and reinforcement of piers.

h_c (m)	Middle and Side Span LRBs ($)	Only Middle Span LRBs ($)
4.60	81300	38360
7.10	86890	40770
9.60	103160	49700

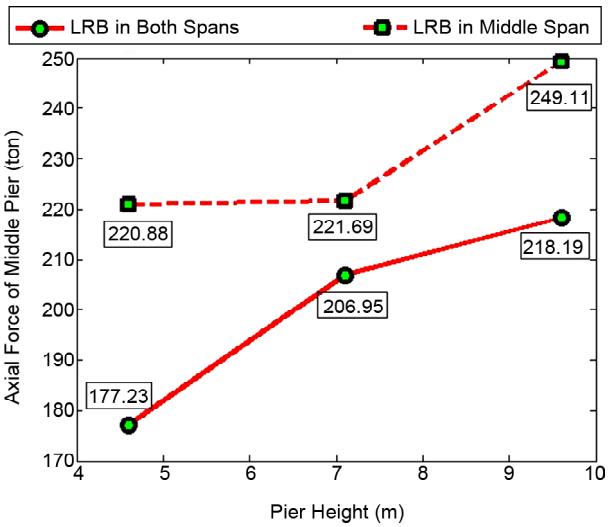

Figure 5. The axial force of middle piers.

5.3. Results Comparison

Based on the output results;

- Cost of materials used includes isolators, concrete and reinforcement of piers reduces by less than half in the case of using LRB isolators in the middle span compared to the cost of using isolators in both middle and side spans (Tables 11 and 12).
- Effective stiffness of middle span LRB isolators in the case of using LRBs at the middle and side spans compared with the use of LRB isolators just at the middle span has increased at the piers height of short and decreased at the height of medium and long.
- For all heights, lead rubber diameter in the case of using LRBs just at the middle span has increased.
- Displacements of the middle LRB isolators in the case of using LRB isolators only in the middle span decreased in the piers height of short and medium and stayed almost equal for a height of long.
- Yield displacement of the middle LRB isolators in case of using LRB isolators only in the middle span is increased in all of the piers height

Table 12. The total cost ratio for use of the middle span LRBs to the use of middle and side spans LRBs.

h_c (m)	Cost Ratio for Middle Span to Middle and Side Span LRBs
4.60	0.47
7.10	0.47
9.60	0.48

- The design forces of side and middle piers of bents in case of using LRB isolators only in the middle span, has increased for axial compression force and decreased for biaxial bending moments.

For the graphical representation of the values shown in the tables, in the Figures (4) to (10), a graphic comparison of several items including the optimal LRBs lead core diameter, the pier diameter, the total diameter of the optimal isolators, the number of LRB rubber layers in the middle span, the displacement of middle span LRB, the design axial force of middle pier and the design biaxial bending moment of middle pier is presented in both cases of using LRBs in the middle and side spans and using LRBs in the middle span.

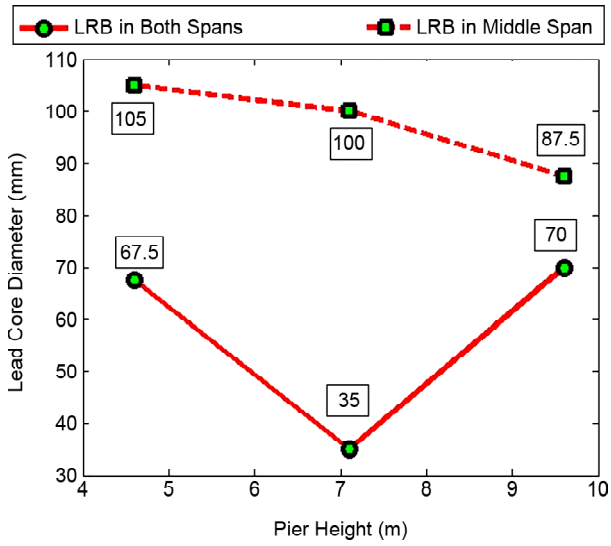

Figure 6. The optimal LRBs lead core diameter.

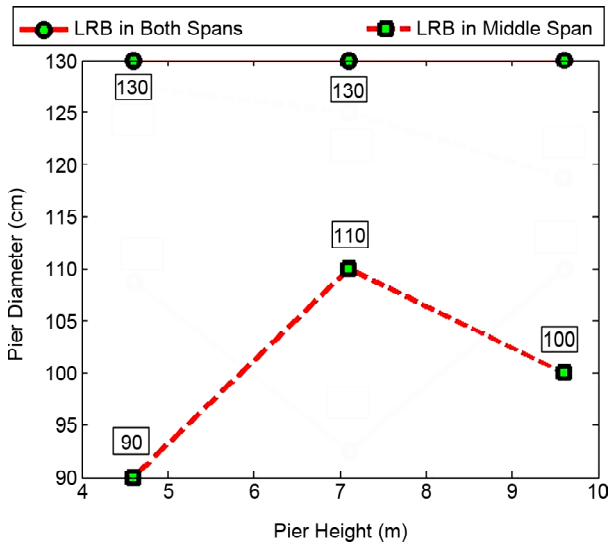

Figure 7. The piers diameter.

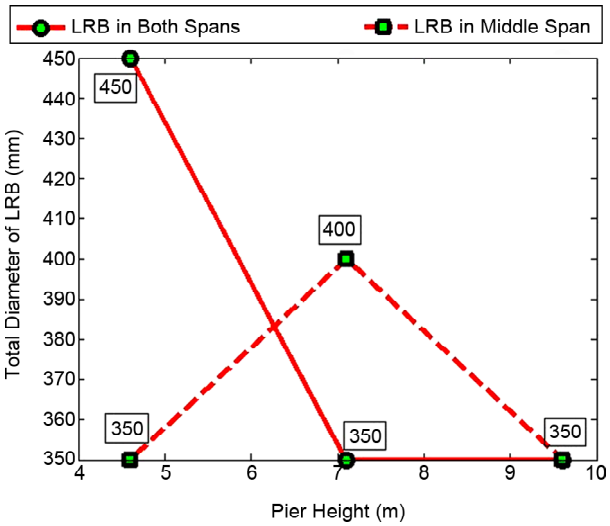

Figure 8. The total diameter of the optimal isolators.

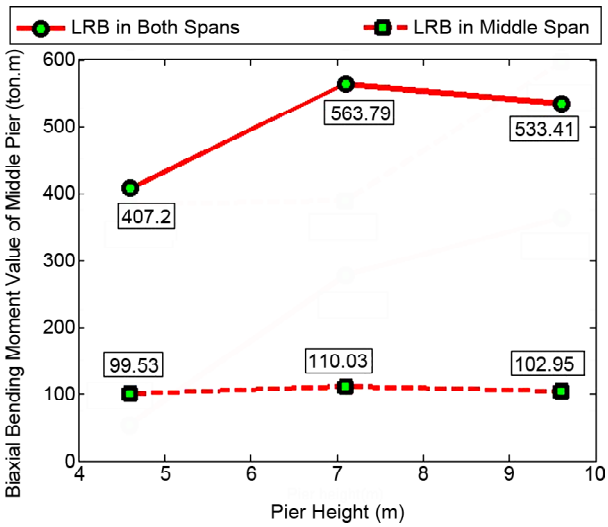

Figure 10. The biaxial bending moment of middle piers.

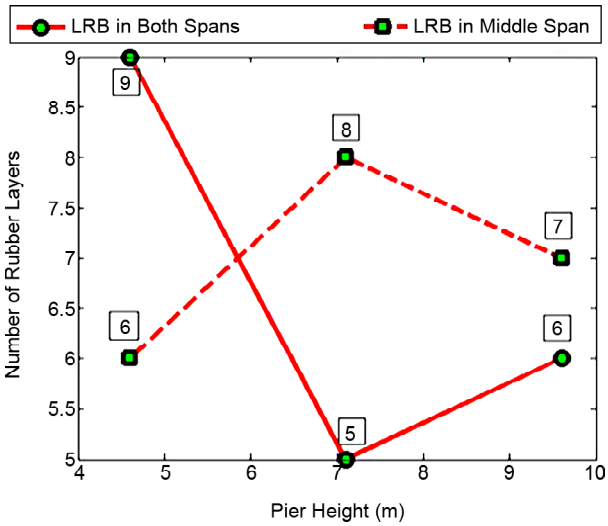

Figure 9. The number of LRB rubber layers.

According to Figures (4) to (10), by removing the isolator of the side spans, the following results are noticeable in the middle span optimum LRB isolators: the diameter of the optimum LRB lead core is increased, the diameter of the piers is reduced, the total diameter of the optimal isolators in short and long piers height is reduced and the number of LRB rubber layers in medium and long piers height is increased.

Therefore, it is clear that the major design forces have been transferred to the abutments.

Also in the Table (13), the design stress ratios (existing stress to allowable stress) are listed based on the formulas of the AASHTO LRFD (top ten

Figure 13. The design stress ratios based on the referred regulations.

Item	Both Spans 4.60 m	Both Spans 7.10 m	Both Spans 9.60 m	Both Spans 4.60 m	Both Spans 7.10 m	Both Spans 9.60 m	Mid. Span 4.60 m	Mid. Span 7.10 m	Mid. Span 9.60 m
	Mid LRB	Mid LRB	Mid LRB	Side LRB	Side LRB	Side LRB	Mid LRB	Mid LRB	Mid LRB
14.7.6.3.2-1	0.36	0.59	0.61	0.70	0.74	0.78	0.64	0.48	0.62
14.7.5.3.2-2	0.38	0.52	0.55	0.18	0.25	0.26	0.62	0.58	0.58
14.7.5.3.5-4	0.33	0.18	0.23	0.29	0.30	0.31	0.26	0.57	0.29
14.7.5.3.5-5	0.19	0.27	0.28	0.64	0.44	0.31	0.31	0.29	0.29
14.7.5.3.2-1	0.44	0.89	0.79	0.41	0.38	0.38	0.93	0.56	0.92
14.7.5.3.3-1	0.25	0.39	0.39	0.23	0.24	0.26	0.43	0.36	0.41
14.7.5.3.3-2	0.16	0.22	0.23	0.02	0.07	0.07	0.26	0.24	0.24
14.7.5.3.6-1	0.22	0.10	0.15	0.53	0.53	0.53	0.16	0.33	0.20
Article 4.5 M251	0.40	0.53	0.53	0.21	0.21	0.22	0.53	0.40	0.53
14.7.5.3.5-1,2	0.16	0.24	0.24	0.05	0.06	0.06	0.26	0.21	0.25
9.5.1.2.1	0.10	0.07	0.08	0.26	0.34	0.33	0.08	0.14	0.09
9.40	0.59	0.41	0.47	0.38	0.57	0.53	0.46	0.83	0.56
9.43	0.52	0.53	0.55	0.39	0.60	0.56	0.05	0.02	0.02

Figure 14. The values of the displacement of LRB isolators.

h_c (m)	Middle and Side Spans Model		Middle Span Model	Primary Model
	Displacement of Middle LRB (mm)	Displacement of Side LRB (mm)	Displacement of Middle LRB (mm)	Deck (mm)
4.60	120.68	50.62	74.84	100-150
7.10	98.01	55.19	86.04	-
9.60	92.54	47.59	93.04	-

rows) and FHWA-NHI 130093 (three lower rows) regulations for optimal isolators in each height of the pier. Studying the table values indicates the proper stress ratios compared to the design values for all optimized LRB isolators.

Finally, in the Table (14), the values of the displacement of middle and side spans in the following three cases are summarized and compared; primary model, model with optimized LRB isolators in the middle and side spans and model with optimized LRB isolators in the middle span.

Finally, in Table (14), the values of the displacement of middle and side spans in the following three cases are summarized and compared; primary model, model with optimized LRB isolators in the middle and side spans and model with optimized LRB isolators in the middle span.

It should be noted that the result of the displacement of the primary model is based on the reference provisions [18] for the El Centro earthquake.

6. Computational Effort

Communication of computational software (CS_i Bridge) and statistical mathematical software (MATLAB 2016) is achieved by an analysis engine in a powerful computer with Core i7 Intel CPU and 12 G Ram, each run taking about 25 hours. At this stage, to achieve the optimal solution for LRB isolators at bents and abutments, a maximum of seven repetitions are needed for each population to converge. For each generation, 50 populations are considered. To determine the sensitivity of the software to the number of generations, initially the number of generations is considered 100 times bigger than the number of variables, which was the software default. However, the minimized objective results were achieved by three times the number of variables. Therefore, to avoid conducting time-consuming and unnecessary calculations, the numerical value of three times the number of variables is used for the number of generations in the following runs. At each execution, nearly 7350 analyses were performed.

All files required for analysis, design, controls, constraints and optimization are under MATLAB software. In the main file, CSi bridge software is opened. The initial file of the isolated bridge with different structural elements is read, including the isolators with the initial computational stiffness, and the values of forces and displacements, etc. are calculated. Modified spectrum analysis was applied corresponding to the construction site and selected variables. These values are used in subsequent MATLAB files to design piers and isolators based on the design method mentioned. Optimization is based on the objective function and design constraints to achieve the minimum cost. All the mentioned steps are done automatically.

7. Conclusion

In this article, a multi-span simply supported highway bridge was optimally designed following AASHTO specifications and by using Lead-Rubber Bearing (LRB) isolators. An earlier researcher previously designed the bridge without the utilization of LRBs. The re-design of the bridge was conducted here by using LRBs and an optimization study based on the Genetic Algorithm (GA). Optimization process aimed at minimizing construction costs consisting of LRB and pier costs and concentrated on the optimal determination of LRB properties and pier dimensions. The case-study on the utilization of LRBs in optimal design of highway bridges indicated the effectiveness of these isolators in reducing construction costs of the class of bridges represented by the studied case. In addition to this indication, studying the mechanical properties of LRBs placed at various positions and on piers with varying heights revealed the following points:

1. The optimization study at all heights in the case of using LRB isolators in middle and side spans is conducted by increasing the stiffness of side

spans to middle span LRB isolators to comply with provisions of the design and the cost function. Results represent a decrease in the effective stiffness ratio of the side spans to middle span LRB isolators as pier height increased by about 30 to 50 percent.

2. The optimization results show that by increasing the height of piers, effective stiffness values of middle span LRB isolators have decreased by about 10 to 20 percent when using LRBs only at the middle span, and increased by about 30 to 50 percent in the case of using LRBs at both middle and side spans.
3. The optimization results show that the pier's diameter optimum values have decreased by about 15 to 30 percent when LRBs have been used just at the middle span.
4. The numerical values of the design forces at the side piers are usually greater than middle piers by about 5 to 10 percent.
5. In the majority of cases, increasing the numerical values of the piers height increases the values of piers design forces by about 5 to 10 percent. Moreover, the percentage of designed reinforcement increases according to the same optimum cross-sectional area of piers in the optimization process by about 40 to 50 percent.
6. By increasing the pier height, the maximum displacement of optimized LRB isolators is usually reduced in the case of using LRBs at the middle and side spans by about 20 percent and increased in the case of using LRBs at the middle span by about 20 percent.
7. The cost of materials used reduces by less than half in the case of using LRB isolators only in the middle span.
8. Using LRBs at the middle span cause biaxial bending moment values of piers reduction in tall side piers by about 40 percent. It is clear that the major design forces have been transferred to the abutments.
9. The shear and flexural properties of the pier on which the LRB resides have a determining effect on the LRB response and its effectiveness in mitigating seismic demand of the bridge.
10. Seeing the LRB-pier combination as a "series" system, a larger part of the system deformation is absorbed by the softer member. Thus, an excessively deformable pier will prevent the LRB from undergoing displacements that are large enough to contribute to absorbing the input vibration.
11. Both too long and too short piers suffer from the excessive deformability mentioned in the previous statement. For short piers, high shear forces produced to withstand the applied bending moments are in charge of the large lateral deformations. For long piers, on the other hand, the small flexural stiffness should be taken responsible for increased lateral deformations.
12. When LRBs excluded from side bearings supported on abutments, smaller bending moment demands experienced by the isolated inner piers by about 75 percent. That is, the enlarged stiffness provided at abutments helps in the absorbance of larger forces by these supports. This results in a remarkable reduction of construction costs due to i) deletion of side LRBs and ii) reduced demand at internal piers and LRBs by about 50 percent.

Finally, for the bridge considered in this study, it is concluded that, in general terms, the optimized value of the designed bridge can be achieved at a lower cost, by middle span deck-isolation compared to middle and side spans deck-isolation.

References

1. Han, R., Li, Y., and van de Lindt, J. (2014) Seismic risk of base isolated non-ductile reinforced concrete buildings considering uncertainties and main shock-aftershock sequences. *Structural Safety*, **50**, 39-56, DOI: 10.1016/j.strusafe.2014.03.010.

2. Bakhshi, A. and Mostafavi, S.A. (2014) Development of fragility curves for base isolated RC structures. *Proceeding of the 9th International Conference on Structural Dynamics*, EURODYN 2014, Porto, Portugal, 2947-2953.

3. Ramanathan, K., Padgett, J.E., and DesRoches, R. (2015) Temporal evolution of seismic fragility curves for concrete box-girder bridges in California. *Engineering Structures*, **97**, 29-46, DOI: 10.1016/j.engstruct.2015.03.069.

4. Shahria Alam, M., Rahman Bhuiyan, M.A., and

Muntasir Billah, A.H.M. (2012) Seismic fragility assessment of SMA-bar restrained multi-span continuous highway bridge isolated by different laminated rubber bearings in medium to strong seismic risk zones. *Bulletin of Earthquake Engineering*, **10**, 1885-1909, DOI: 10.1007/s10518-012-9381-8.

5. Asadi, P. (2019) Neighbour matrix for optimal seismic design of RC frames for minimum total life-cycle cost. *Journal of Seismology and Earthquake Engineering*, **21**(2), 77-87.

6. Kumar Roy, B. and Chakraborty, S. (2015) Robust optimum design of base isolation system in seismic vibration control of structures under random system parameters. *Structural Safety*, **55**, 49-59, DOI: 10.1016/j.strusafe.2015.02.005.

7. Moghaddam, H. and Hosseini Gelekolai, S.M. (2017) Optimum seismic design of short to mid-rise steel moment resisting frames based on uniform deformation theory. *Journal of Seismology and Earthquake Engineering*, **19**(1), 13-24.

8. Jensen, H.A., Mayorga, F., and Valdebenito, M.A. (2015) Reliability sensitivity estimation of nonlinear structural systems under stochastic excitation: A simulation-based approach, Comput. *Methods Appl. Mech. Engrg.*, **289**, 1-23, DOI: 10.1016/j.cma.2015.01.012.

9. Pourzeynali, S. and Zarif, M. (2008) Multi-objective optimization of seismically isolated high-rise building structures using genetic algorithms. *Journal of Sound and Vibration*, **311**, 1141-1160, DOI: 10.1016/j.jsv.2007.10.008.

10. Chisari, C., Bedon, C., and Amadio, C. (2015) Dynamic and static identification of base-isolated bridges using Genetic Algorithms. *Engineering Structures*, **102**, 80-92, DOI: 10.1016/j.engstruct.2015.07.043.

11. Ozdemir, G., Avsar, O., and Bayhan, B. (2011) Change in response of bridges isolated with LRBs due to lead core heating. *Soil Dynamics and Earthquake Engineering*, **31**, 921-929, DOI: 10.1016/j.soildyn.2011.01.012.

12. Hedayati Dezfuli, F., and Shahria Alam, M. (2013) Multi-criteria optimization and seismic performance assessment of carbon FRP-based elastomeric isolator. *Engineering Structures*, **49**, 525-540, DOI: 10.1016/j.engstruct.2012.10.028.

13. Lute, V., Upadhyay, A., and Singh, K.K. (2011) Genetic algorithms-based optimization of cable stayed bridges. *Journal of Software Engineering and Applications*, **4**, 571-578, DOI: 10.4236/jsea.2011.410066.

14. Fallah, N. and Zamiri, G. (2013) Multi-objective optimal design of sliding base isolation using genetic algorithm. *Scientia Iranica A*, **20**(1), 87-96, DOI: 10.1016/j.scient.2012.11.004.

15. Hameed, A., Koo, M.S., Do, T.D., and Jeong, J.H. (2008) Effect of lead rubber bearing characteristics on the response of seismic-iso-lated bridges. *KSCE Journal of Civil Engineering*, **12**(3), 187-196, DOI: 10.1007/s12205-008-0187-9.

16. Bessason, B. and Haflidason, E. (2004) Recorded and numerical strong motion response of a base-isolated bridge. *Earthquake Spectra*, **20**(2), 309-332, DOI: 10.1193/1.1705656.

17. Liao, W.I., Loh, C.H., and Lee, B.H. (2004) Comparison of dynamic response of isolated and non-isolated continuous girder bridges subjected to near-fault ground motions. *Engineering Structures*, **26**, 2173-2183, DOI: 10.1016/j.engstruct.2004.07.016.

18. Nielson, B.G. (2005) *Analytical Fragility Curves for Highway Bridges in Moderate Seismic Zones*. Georgia Institute of Technology.

19. U.S. Department of Transportation (2014) *LRFD Seismic Analysis and Design of Bridges (Reference Manual)*, Publication No. FHWA-NHI-15-004.

20. MATLAB and Statistics Toolbox R2016a. The MathWorks, Inc., Natick, Massachusetts, the United States.

21. CSi Bridge Ver. 16 software, *Computers and Structures*, Inc., United States.

Appendix A. Determine the main characteristics of LRB isolator

Characteristic strength of LRB isolator Q_d (in Newton) can be calculated by Equation (A.1):

$$Q_d = 6.3585 d_L^2 \tag{A.1}$$

That lead core diameter *dL* is in millimeters. In addition, the calculation of effective stiffness of the isolator (K_{eff}) is done by Equation (A.2):

$$K_{eff} = \frac{F_{\max}}{\Delta_{\max}} = \frac{Q_d + K_d \Delta_{\max}}{\Delta_{\max}} = \frac{Q_d}{\Delta_{\max}} + K_d \tag{A.2}$$

In which $F_{\max}$ is the maximum shear force (in Newton), $\Delta_{\max}$ maximum isolator displacement (in millimeters) and K_d secondary stiffness of isolator after the yield (in Newton per millimeter).

Damping of the isolator (*h*) will be calculated using the Equation (A.3):

$$h = \frac{2Q_d\left(\Delta_{\max} - \Delta_y\right)}{\pi K_{eff} {\Delta_{\max}}^2} = \frac{2Q_d}{\pi F}\left(1 - \frac{\Delta_y}{\Delta_{\max}}\right) \tag{A.3}$$

Δ_y is displacement at yield point of isolator in millimeters.

Effective period of isolation system (in seconds) is determined by using the following equation:

$$T_{eff} = 2\pi\sqrt{\frac{W}{K_{eff} g}} \tag{A.4}$$

In which W is the total weight of the superstructure of the bridge (in Newton), g is the acceleration of gravity (in meters per second squared).

Appendix B. Characterize the Design Spectrum Used in the LRB Isolation Design

Having the PGA, S_S and S_1 on the site, F_a, F_v and FPGA coefficient values are calculated based on soil conditions of Table 2-4 and Table 2-5 in the corresponding reference 1. Then we have:

$$A_S = F_{PGA} PGA \tag{B.1}$$

$$S_{DS} = F_a S_S \tag{B.2}$$

$$S_{D1} = F_v S_1 \tag{B.3}$$

$$T_S = \frac{S_{D1}}{S_{DS}} \tag{B.4}$$

$$T_0 = 0.2 T_S \tag{B.5}$$

$$C_{sm} = A_S + \left(S_{DS} - A_S\right)\left(T_m / T_0\right) \tag{B.6}$$

By using the Equation and conditions below, modification of the design spectrum is carried out at high periods:

$$\text{if } T > 0.8 T_{eff} \Rightarrow B = \frac{S}{B_L}$$

where

$$B_L = \left(\frac{h}{0.05}\right)^{0.3} \tag{B.7}$$

The values used for the formation of the spectrum design are given in the Table (B.1).

Table B.1. Required values for formation of the design spectrum.

PGA	S_S	S_1
0.35g	0.7899	0.2664